Journal of Research in Pharmacy
Research Article
www.jrespharm.com

Effects of lesinurad on HEK-293 human kidney cells: *In vitro* and molecular docking evaluation

Tugce BORAN[1,2 ¥*], Mahmoud ABUDAYYAK[1 ¥], Mohammed T. QAOUD[3,4]

1 Department of Pharmaceutical Toxicology, Faculty of Pharmacy, Istanbul University, Istanbul, Turkey.
2 Department of Pharmaceutical Toxicology, Faculty of Pharmacy, Istanbul University-Cerrahpaşa, Istanbul, Turkey
3 Department of Pharmacy, Faculty of Pharmacy, Cyprus International University, Nicosia, Northern Cyprus, Turkey
4 Department of Pharmaceutical Chemistry, Faculty of Pharmacy, Gazi University, 06330. Etiler, Ankara, Turkey

* Corresponding Author. E-mail: boranntugce@gmail.com (T.B.); Tel. +09-212-866 37 00.
¥ Both Boran T and Abudayyak M contributed equally as the first authors.

Received: 12 April 2023 / Revised: 26 September 2023 / Accepted: 27 September 2023

ABSTRACT: Lesinurad is a drug used for the treatment of hyperuricemia. It has been reported that lesinurad causes renal adverse events. The molecular effects of lesinurad in the kidney cells have not been elucidated clearly. The embryonic kidney cells (HEK-293) were treated with lesinurad at various concentrations (12.5-100 µM) for 24h. The cytotoxicity, apoptotic effect, reactive oxygen species (ROS), lipid peroxidation (MDA), and total antioxidant capacity (TAC) levels were evaluated. Secretion of the inflammatory mediators was examined after lesinurad treatment. Additionally, molecular docking studies were performed for lesinurad with TNF-α and concanavalin a (ConA). Lesinurad did not induce apoptotic cell death at the tested concentrations. The ROS and MDA levels insignificantly declined, and the TAC level increased. TNF-α secretion was induced after 100 µM lesinurad treatment. Lesinurad significantly decreased the Con a-induced inflammatory mediators' secretion. The docking studies results show a weak interaction with TNF-α but strong interaction with Con a proteins. These findings support that lesinurad-induced kidney toxicity could be related to the mechanical stress of uric acid crystals rather than the induction of inflammation by the initiation of oxidative damage.

KEYWORDS: Lesinurad-1; nephrotoxicity-2; inflammation-3; urate-lowering therapy -4; molecular docking-5.

1. INTRODUCTION

Hyperuricemia is one of the main causes of gout and can also be a risk factor in the development of cardiovascular diseases and metabolic syndrome [1]. Lesinurad is a new urate-lowering medicine, that inhibits organic anion transporter 4 (OAT4) and uric acid transporter 1 (URAT1) and reduces the reabsorption of uric acid from the kidneys as it has been shown that lesinurad potently inhibits uric acid transporters than other urate-lowering drugs (probenecid), which makes it important for the treatment of gout patients [2]. It was approved by the Food and Drug Administration (FDA) and European Medicines Agency (EMA) for hyperuricemia treatment in combination with xanthine oxidase inhibitors, but not alone, in patients who cannot be treated adequately with allopurinol alone [3,4]. The most common lesinurad-induced adverse reactions are an increase in blood creatinine levels, influenza, gastroesophageal reflux, and headache [5]. Additionally, it has black box warnings about renal injury as acute kidney injury cases have been reported following lesinurad therapy, it has been stated acute kidney injury risk elevates as the dose of lesinurad increases [3,6,7]. It has been thought that the nephrotoxic effects of lesinurad may be associated with uric acid crystallization in the kidney since uric acid transport inhibition leads to the accumulation of uric acid and crystallization [8]. However, this mechanism has not been confirmed by clinical and experimental studies [9].

This study aimed to investigate the role of oxidative stress and inflammatory effects in lesinurad-induced nephrotoxicity. For that, besides the cytotoxicity and apoptotic effect, the changes in the levels of reactive oxygen species (ROS), lipid peroxidation (MDA), total antioxidant capacity (TAC), and

How to cite this article: Boran T, Abudayyak M, Qaoud MT, Effects of lesinurad on HEK-293 human kidney cells: In vitro and molecular docking evaluation. J Res Pharm. 2024; 28(3): 708-721.

http://dx.doi.org/10.29228/jrp.733
ISSN: 2630-6344

inflammatory mediators were evaluated using human embryonic epithelial cell line (HEK-293). HEK-293 cells are a human-originated and well-characterized cell line used as a model for investigating nephrotoxicity in humans [10-12].

As the lesinurad caused a significant decrease in the pro-inflammatory cytokine, tumor necrosis factor (TNF) –α, which is produced primarily by activated macrophages and monocytes [13,14]. A variety of inflammatory diseases such as diabetes, rheumatoid arthritis (RA), multiple sclerosis and atherosclerosis, ulcerative colitis, and Crohn's disease are usually associated with a high level of TNF-α. In the presence of TNF-α converting enzyme (TACE), a membrane-bound zinc metalloprotease enzyme, the pro-TNF-α is converted into the soluble and active form of TNF-α [15]. Thus, the mechanism of reducing the TNF-α level was proposed to be a result of inhibiting the TACE enzyme.

Concanavalin a (Con a) is a plant lectin (carbohydrate-binding protein) and it is extracted from the jack bean (Canavalia ensiformis). Con a could affect many physiological pathways such as agglutination [16], lymphocyte mitogenesis [17], and stimulation of several matrix metalloproteinases (MMPs) [18]. Con a has been shown to eradicate hepatic tumors in the murine model through activation of the immune response in the liver [19]. As the effect of Con a was also significantly reduced as a result of treating HEK-293 with lesinurad, it was suggested that the drug has some affinity toward Con a resulting in decreasing in the Con a effects. Therefore, molecular docking studies were applied to investigate the potential of these assumptions.

2. RESULTS

2.1. Cytotoxicity of lesinurad on the kidney cells

Cell viability was decreased in a dose-dependent manner. The cell death was significant at concentrations higher than 100 µM, the IC_{50} value of lesinurad was calculated to be 302.51 µM. At 100 µM concentration, cell viability was determined to be more than 80%. To evaluate the possible death pathway, an annexin V /PI kit was used. The results show that lesinurad did not induce apoptotic cell death in the HEK-293 cell line at the tested concentrations (p>0.05) (Figure 1).

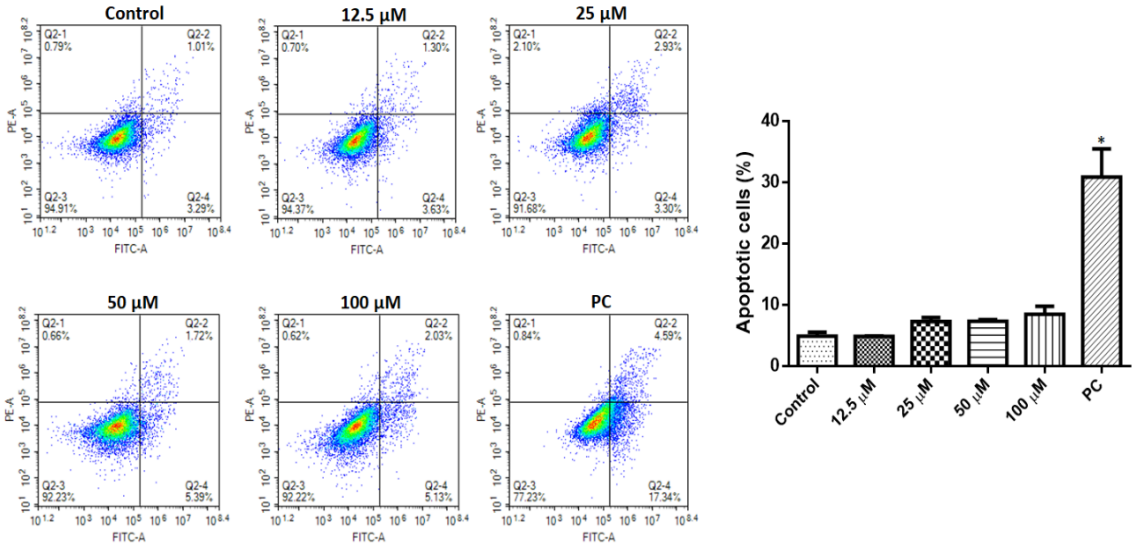

Figure 1. Apoptotic effect of lesinurad after 24 h exposure. PC: positive control (500 µM H_2O_2). The cells exposed to 1% DMSO were accepted as the control group *p<0.05 calculated versus the control group

2.2. Oxidative stress versus antioxidant effect

Although 24 h of exposure to lesinurad induced a decrease in ROS and MDA levels and an increase in TAC level the changes were insignificant (p> 0.05) (Figure 2).

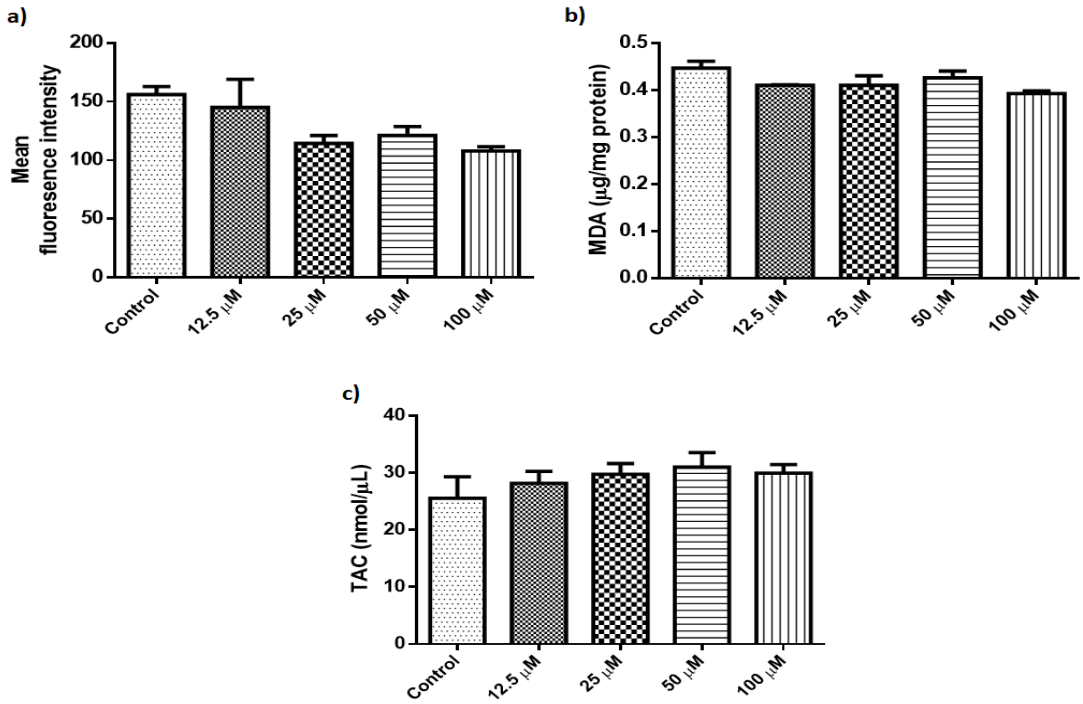

Figure 2. Oxidative effects of lesinurad on HEK-293 kidney cells a) Mean fluorescence intensity of DCF^+ cells b) MDA level and c) TAC level in the cells.

2.3. NF-κB protein level

Following 24 h lesinurad treatment, NF-κB protein expression dose-dependently was decreased, however, the decrease was found to be statistically significant only at the 100 µM concentration group (Figure 3).

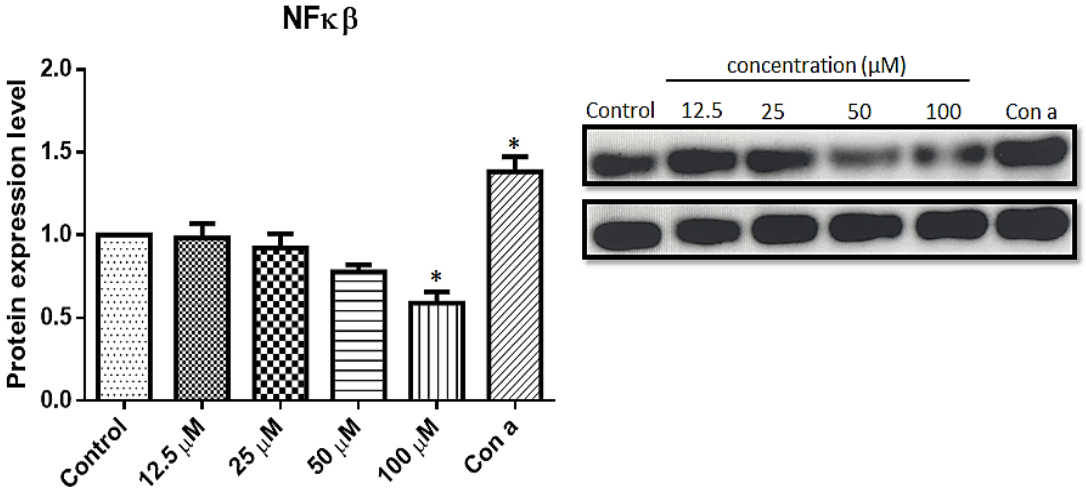

Figure 3. NF-κB protein expression level in HEK-293 kidney cell line after 24 h lesinurad exposure. *p<0.05 versus the control group. NF-κB: Nuclear Factor kappa B. Con a: Conconavalin a.

2.4. Changes in inflammatory mediators

While lesinurad did not induce any increase in TNF-α, IL-10, IL-6, and IL-2 levels, it decreased the levels of IL-6 and TNF-α in HEK-293 kidney cells, this decrease was significant only for TNF-α at the highest concentration. 100 µM was chosen to assess the anti-inflammatory effect of lesinurad. Results showed that lesinurad significantly (p<0.05) inhibited the secretion of TNF-α, IL-10, IL-6, and IL-2 in the cells pre-exposed to Con a (25 µg/mL) (Figures 4 and 5).

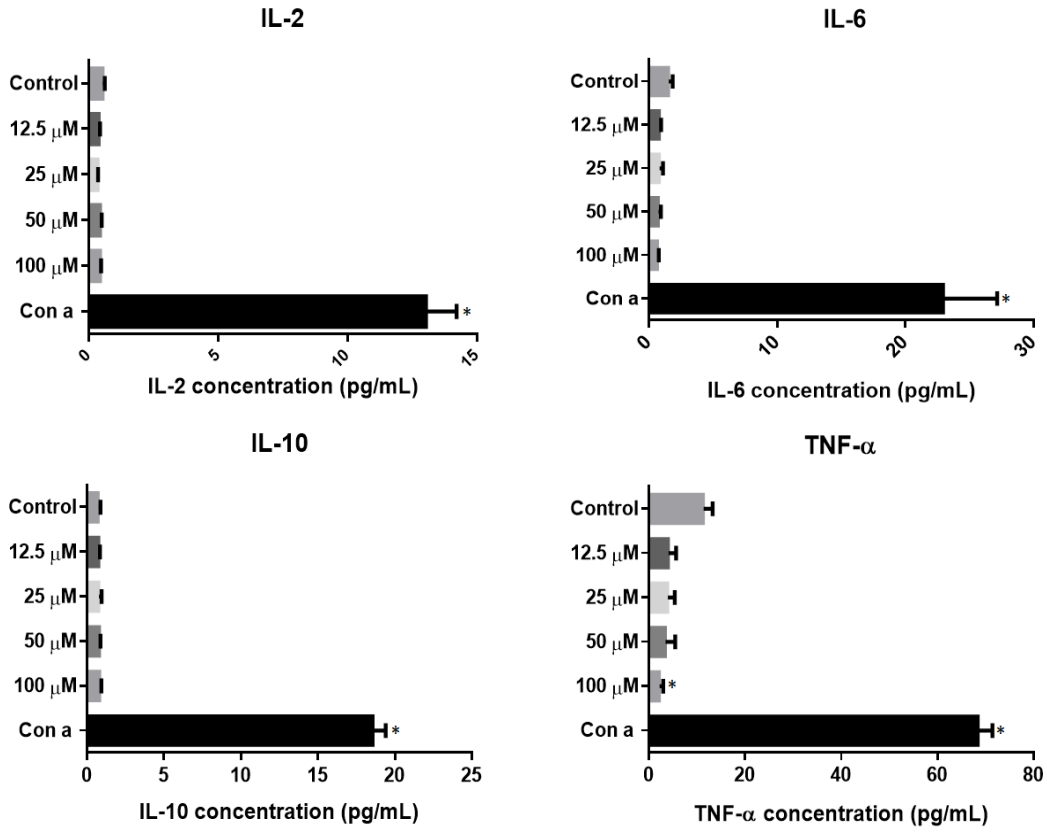

Figure 4. Changes of cytokine levels in HEK-293 kidney cell line after 24 h lesinurad treatment. *p<0.05 versus the control group. IL: interleukin, TNF-α: tumor necrosis factor-alpha. Con a was used as a positive control.

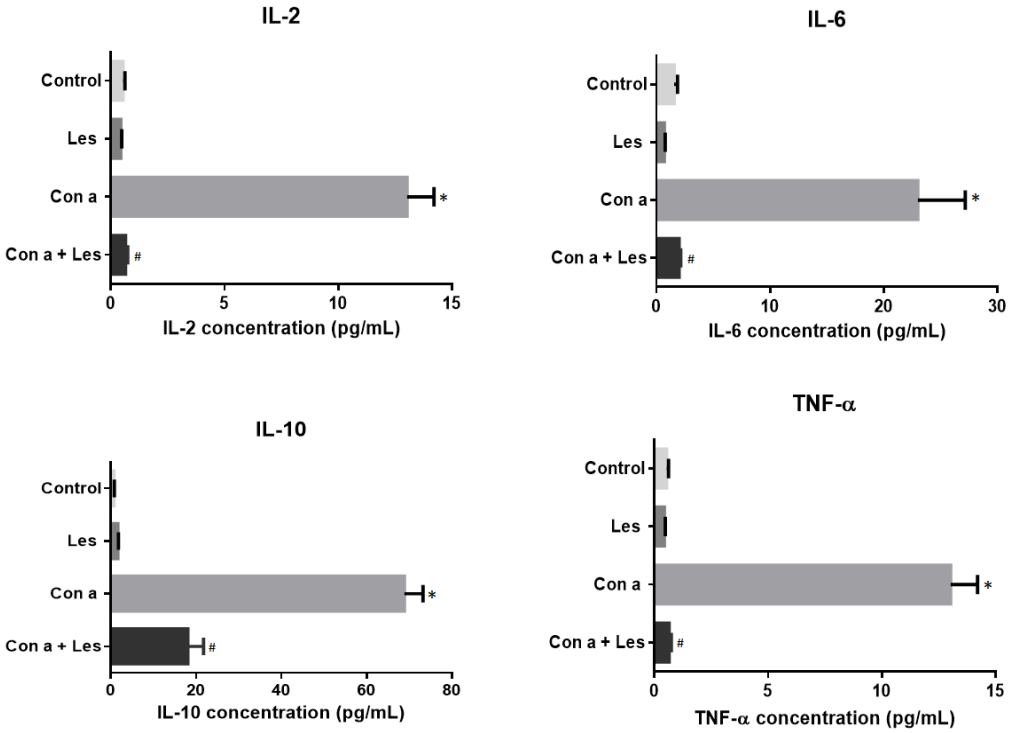

Figure 5. Anti-inflammatory effect of lesinurad (100 µM, 24 h) on HEK-293 kidney cells pre-treated with Con a for 12 h. *p<0.05 versus control group, #p<0.05 versus Con a group.

2.5. Molecular Docking and MM-GBSA Studies

In order to verify the accuracy of the applied molecular docking procedure for each protein structure, the rebuilt and resulting docked poses for each native ligand were aligned on the respective co-crystallized ligand using the superimposition tool in the Maestro program, and the root mean square deviation (RMSD) values were calculated (Figure 6). The RMSD values were determined to be 0.457 for ik-682, the native ligand of TACE crystal structure (PDB code: 2FV5), and 0.964 for α-methyl-D-mannopyranoside, the native ligand of concanavalin A crystal structure (PDB code: 5CNA). These observed RMSD values fall within the acceptable range of being lower than 2Å. Therefore, it can be concluded that the docking process was performed accurately and can be considered reliable for the studied ligands.

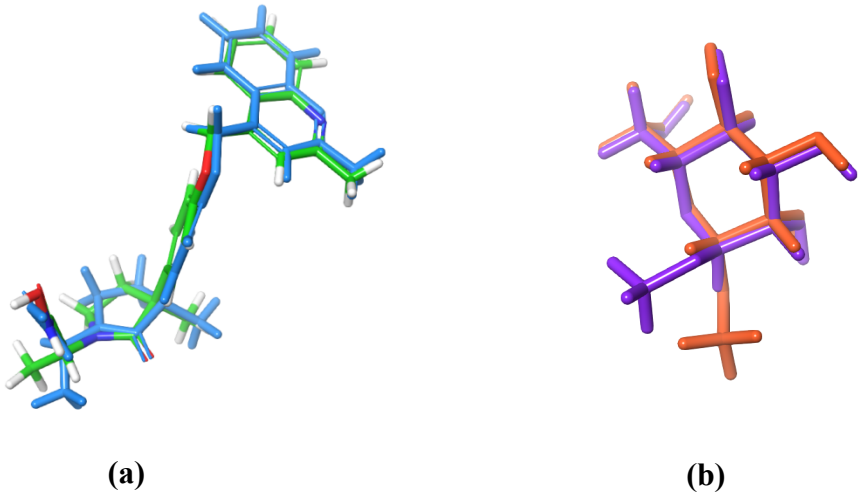

Figure 6. Superimposition of the reduced docked form and the crystal form of the native ligands: (a) ik-682, the native ligand of TACE (PDB ID: 2FV5), and (b) α-methyl-D-mannopyranoside, the native ligand of concanavalin A (PDB ID: 5CNA).

From the docking results, it is evident that lesinurad exhibited a lower docking score (-3.46 kcal/mol) compared to the reference structure (ik-682), which had a docking score of -12.52 kcal/mol. Analyzing the docking studies on the TACE protein, it is obvious that the zinc ion and specific amino acid residues, namely Gly-349, Leu-348, and Glu-406, play a significant role in the inhibitory activity of TACE. These residues form six valuable hydrogen bonds within the binding site, suggesting their importance in the binding and potential inhibition of TACE. As depicted in Figure 7-a, ik-682 exhibits optimal positioning within the binding site, and its high affinity is primarily attributed to several key interactions. Specifically, it forms two hydrogen bonds with Gly-349, one hydrogen bond with Leu-348, and the hydroxyl group forms a hydrogen bond with Glu-406. In addition, ik-682 forms a coordination bond with the zinc ion, and the zinc also participates in another coordination bond with the carbonyl oxygen of the hydroxamine group. Furthermore, a pi-cation interaction occurs between the zinc and the phenyl ring of ik-682. These favorable interactions are complemented by various hydrophobic interactions involving Tyr347, Leu348, Glu-398, Leu-401, His-405, Ala-439, Val-440, and Asn-447 [20]. On the contrary, docking of lesinurad to the TACE binding site reveals the formation of only two hydrogen bonds with TYR-390 and a surrounding water molecule. Unlike ik-682, lesinurad does not exhibit favorable interactions with the zinc ion and other important amino acids observed previously. As depicted in Figure 7-b, the presence of the bulky cyclopropyl-naphthalene ring in lesinurad causes the bromo-triazole ring to be pushed outside the binding site. This results in steric clashes and ultimately leads to the observation of weak to moderate affinity for lesinurad.

(a)

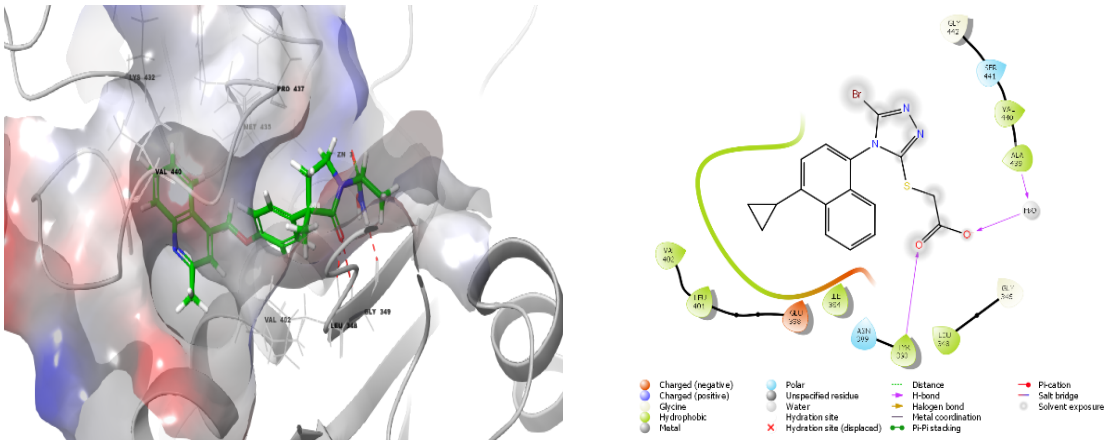

(b)

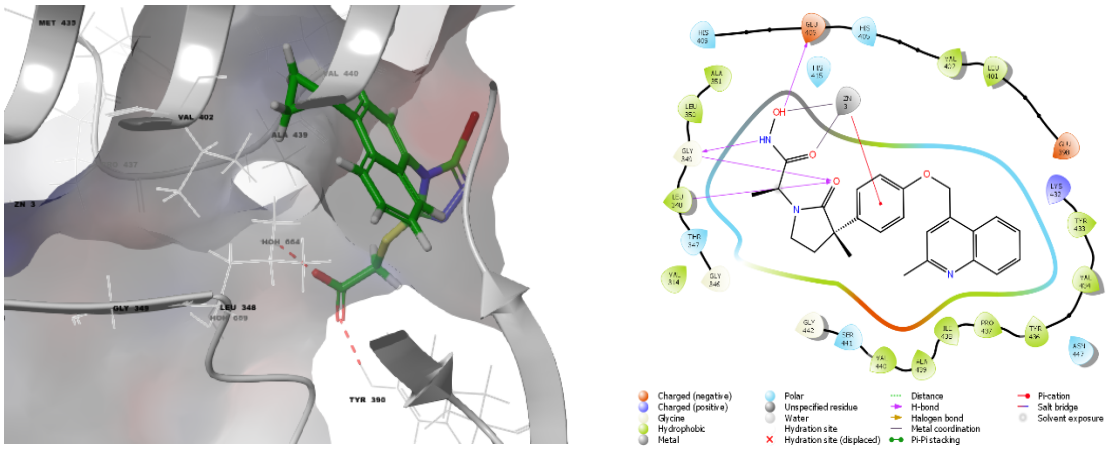

Figure 7. Docking mode of ik-682 (a) and lesinurad (b) into the active site of TACE (PDB code: 2FV5) shown in 2D and 3D views. The binding site is mapped as an electrostatic potential surface, where red and blue indicate areas of negative and positive electrostatic potential, respectively (transparency set to 70%). In the 3D structure, the ligands are represented as green stick structures. The Hydrogen bonding, salt bridge, and π-cationic interactions are denoted by red, purple, and green dotted lines.

Within the carbohydrate-binding site of the Con a protein, the reference ligand α-methyl-D-mannopyranoside (α-MeMP) exhibits higher affinity compared to the drug lesinurad. The α-MeMP aligns ideally within the binding pocket. The calculated docking score for α-MeMP is -6.97, indicating a strong binding affinity. Furthermore, the MM-GBSA value for α-methyl-D-mannopyranoside is -35.2 kcal/mol, further supporting its favorable binding energy. The superior affinity of the reference agent, α-MeMP, can be attributed to the formation of various favorable interactions with nearby amino acid residues. These include Arg-228, Asn-14, Asp-208, Tyr-100, and Leu-99. Additionally, α-MeMP forms an additional hydrogen bond with a nearby water molecule (as depicted in Figure 8-a). These observed interactions align with previously reported results, further confirming their significance in contributing to the strong binding affinity of α-MeMP within the Con a protein's binding site [21]. The docking of lesinurad within the carbohydrate-binding pocket of Con a, as illustrated in Figure 8-b, reveals the presence of several favorable interactions. These interactions include the formation of two salt bridge interactions with Arg-228 and Asn-14. Additionally, lesinurad forms two hydrogen bonds with Arg-228. Notably, Arg-228 is also involved in a pi-cation bond with the triazole ring of lesinurad. These observed interactions highlight the importance of Arg-228 in contributing to the binding of lesinurad within the carbohydrate-binding pocket of Con a. The observed favorable interactions within the carbohydrate-binding pocket of Con a play a significant role in driving a moderate affinity for lesinurad compared to the reference ligand. This is supported by the recorded XP glide docking score of -4.01 and MM-GBSA score of -8.45. Similar to the observations in the TACE protein, the presence of the bulky cyclopropyl-naphthalene group in lesinurad causes the bromo-triazole ring to be pushed outside the binding site. This spatial arrangement leads to a reduction in affinity, as observed in the 3-D view.

Journal of Research in Pharmacy
Research Article

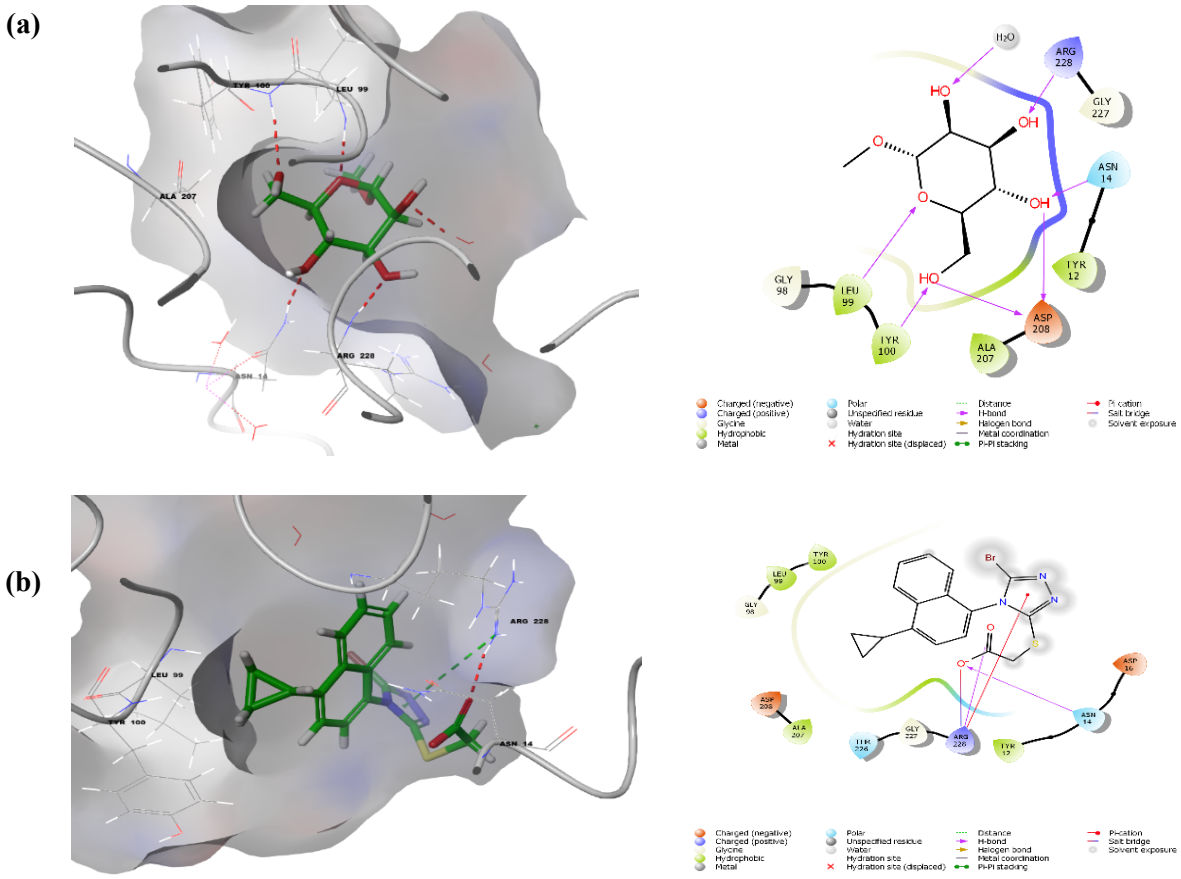

Figure 8. Docking mode of α-methyl-D-mannopyranoside (a) and lesinurad (b) into the active site of Con a (PDB code: 5CNA) shown in 2D and 3D views. The binding site is mapped as an electrostatic potential surface, where red and blue indicate areas of negative and positive electrostatic potential, respectively (transparency set to 70%). In the 3D structure, the ligands are represented as green stick structures. The Hydrogen bonding, salt bridge, and π-cationic interactions are denoted by red, purple, and green dotted lines.

A summary of the obtained XP docking, glide emodel, glide gscore, MM-GBSA scores, as well as the amino acid residues involved in the interaction profiles and the type of interactions, can be found in Table 1.

Table 1. Detailed interactions and binding scores of lesinurad, ik-682, and α-methyl-D-mannopyranoside compounds within the binding pocket of both Con a (PDB ID: 5CNA) and TACE (PDB ID: 2FV5) target proteins.

Con a protein target (PDB ID: 5CNA)		**TACE protein target** (PDB ID: 2FV5)		**Type of interactions**
α-methyl-D-mannopyranoside	**Lesinurad**	**ik-682 comp**	**Lesinurad**	
Asn14, Asp208,Tyr100, Leu99, Arg228	Arg228	Glu406, Gly349, Leu348	Tyr390	**H. Bs**
-	Tyr12, Tyr100, Arg228	Tyr347, Leu348, Glu398, Leu401, His405, Ala439, Val440, Asn447	Leu348, Ile394, Glu398, Leu401, Val402, Ala439	**HPHO**
-6.97	-4.01	-12.52	-3.46	**Docking score**
-6.97	-4.01	-12.54	-3.46	**Glide gscore**
-56.22	-38.03	-147.38	-38.02	**Glide emodel**
-35.2	-8.45	-49.47	-18.97	**MM-GBSA (ΔG)**

H. Bs: hydrogen bond interactions. **π-Cation:** pi-cationic interactions**. HPHO:** hydrophobic interactions.

http://dx.doi.org/10.29228/jrp.733
J Res Pharm 2024; 28(3): 708-721

3. DISCUSSION

Lesinurad and xanthine oxidase inhibitors combination therapy was approved for hyperuricemia patients who cannot be treated adequately with xanthine oxidase inhibitors alone [3,4]. Lesinurad selectively inhibits uric acid transporters and reduces serum uric acid levels. However, in 2019 it was reported that lesinurad was discontinued in the USA because of business reasons, not for efficacy or toxicity issues [22]. One of the main concerns about lesinurad is renal adverse events, and it has a black box warning about acute renal injury [4]. While some previous data indicate that the mechanism of lesinurad may be a consequence of uric acid crystallization in the kidney which could lead to renal injury, this has not been supported by experimental studies [8]; the nephrotoxic effect and so the underlying mechanism of lesinurad is still unclear. Thus, in this study, the renal effects of lesinurad were evaluated using the HEK-293 cell model.

Cytotoxic drugs are among the common causes of hyperuricemia [23] on the same hand, hyperuricemia is associated with cell death through apoptotic effects [24]. While lesinurad is used to decrease concentrations of blood uric acid, it causes to increase in the level of uric acid in the kidney tissue at the same time and this accumulation could lead to renal cell death. Heitel et al. (2018) reported no cytotoxicity of lesinurad at a concentration up to 50 µM [25]; in the current study, the IC_{50} of lesinurad was calculated to be 302.15 µM which is nearly 7-fold of the therapeutic serum's level. The annexin V/PI protocol also shows no significant apoptotic effect of lesinurad at a concentration of up to 100 µM.

Oxidative stress has been shown to increase in gout patients as a result of hyperuricemia and this is a contributing factor to the emergence of renal dysfunction [26, 27]. Besides that, the accumulation of uric acid in the kidney tissue because of treatment with lesinurad is hypothesized to induce oxidative stress in the cells. However, the present research results show that lesinurad did not induce any significant change in ROS or MDA levels and did not affect the antioxidant system as no reduction in TAC levels was noticed. Similarly, Alghamdi et al. (2020) showed that lesinurad diminished plasma MDA levels and increased plasma catalase and glutathione peroxidase levels insignificantly [27]. These results indicate an increase in antioxidant enzymes to estimate the redox balance in the cells without induction of lipid peroxidation.

Chronic and untreated hyperuricemia leads to renal inflammation via activation of the NF-κB signaling pathway [28]. NF-κB is a transcription factor that induces transcription of the other inflammatory factors, so it is one of the main regulators in the development of inflammatory response [29]. In the study, NF-κB protein expression was significantly decreased at 100 µM. additionally, the expression level of TNF-α significantly decreased at the same concentration. TNF-α causes the activation of NF-κB and NF-κB causes the release of TNF-α [30, 31]. The decrease in *NF-κB* expression might be a consequence or a reason for decreases in TNF-α secretion. The slight, but insignificant, decrease in IL-6 supports this assumption; The IL-6 expression is just as TNF- α expression stimulated by NF-κB, and the decrease of IL-6 causes a decrease in NF-κB level. Reduction of IL-6 and TNF-α levels in the kidney has been shown to ameliorate kidney toxicity. Heitel et al. (2018) indicated that lesinurad might exhibit anti-inflammatory effects via peroxisome proliferator-activated receptor gamma (PPARγ) modulator activity on the HEK-293 cell line [25]. Similarly, in this study, lesinurad shows an anti-inflammatory effect as it significantly decreases the levels of IL-10, IL-6, IL-2, and TNF- α in cells pre-treated with Con a, an inflammatory agent, for 12h.

In our study, we aimed to elucidate the in vitro results by investigating the roles of TACE and Con a proteins in modulating TNF-α and inflammatory mediators, respectively, upon exposure to lesinurad. Molecular docking studies were conducted to explore the binding mode and interaction patterns of lesinurad within the binding pockets of TACE and Con a. The significant decrease in TNF-α and inflammatory mediators observed only at a high concentration of lesinurad exposure (100 µM) suggests the low to moderate affinity of lesinurad for both proteins. These findings are supported by the identification of less favorable interactions and binding behavior within the binding sites of TACE and Con a when compared to the reference ligands. Consequently, weaker glide docking scores and MM-GBSA values were observed. These molecular docking results provide valuable insights into the binding characteristics of lesinurad and help explain the observed experimental data. Furthermore, these findings contribute to our understanding of the drug's selectivity, toxicity, and drugs impact on various physiological pathways. This information can be utilized to improve the chemical and physiological properties of lesinurad, enhancing its effectiveness and reducing potential adverse effects.

4. CONCLUSION

In conclusion, the mechanism of lesinurad depends on the reduction of uric acid in the blood by inhibiting the uric acid transporters that are responsible for the reuptake of uric acid from the kidney; Starting from this point of view, it was hypothesized that lesinurad cause to the uric acid accumulation in the kidney cells, which after that induces oxidative stress-related inflammation and cell death. However, lesinurad showed cytotoxicity at levels higher than the therapeutic concentrations (IC_{50} ≥ 7-fold of therapeutic levels), at concentrations up to 100 µM didn't show an elevation in oxidative stress endpoints, depletion in the antioxidant system, nor increases in inflammation markers expressions. Oppositely, lesinurad decreases the levels of inflammation biomarkers after the pre-treatment with an inflammatory agent. Therefore, these results nullify the proposed hypothesis and no relation between lesinurad exposure with inflammation of oxidative stress. The lesinurad- induced acute kidney injury could be associated with mechanical damage because of uric acid crystallization. However, more studies are required to confirm our results.

5. MATERIALS AND METHODS

5.1. Cell Culture and Drug Treatment

HEK-293 cell line was purchased from the American Type Culture Collection (ATCC, USA). HEK-293 cells were cultured in an RPMI cell culture medium containing 10% heat-inactivated fetal bovine serum and 1% antibiotic. The cells were subdivided (sub-cultured) when reach 70% confluence. The culture medium was altered every 2-3 times per week. All experiments were done with the passage between 10-20.

The previous data determined the maximum plasma concentration of lesinurad as 14.84 µM after oral administration of 200 mg lesinurad [4]. Heitel et al (2018) reported no cytotoxicity of lesinurad at concentrations up to 50 µM. In their work to evaluate the effect of lesinurad on CYP 450 enzymes [25], Gillen et al. (2017) used concentrations between 0.16 and 100 µM and calculate the inhibition concentrations to be more than 16.2 µM [32]. Therefore, different concentrations of up to 1000 µM were used to evaluate the cytotoxicity; According to cytotoxicity results and the previous data concentrations between 12.5 µM and– 100 µM were chosen for the other parameters. Following the cellular attachment, cells were exposed to lesinurad for 24 The control groups were treated with a cell culture medium containing 1% DMSO.

5.2. MTT cytotoxicity assay

The cytotoxic effect of lesinurad was evaluated spectrophotometrically using MTT dye (3-(4,5-dimethylthiazol-2-yl)-2,5-diphenyltetrazolium bromide). Viable cells reduced tetrazolium ring to formazan crystals [33]. Briefly, about $1x10^4$ cells/well were seeded into 96 well plates. After lesinurad treatment, MTT dye solution (5 mg/mL) was added to each well and incubated at 37 °C for a further 3 h. Then, the crystals were dissolved in 100 µL of DMSO. Optical density (OD) was read at 590 nm with a microwell plate reader (Epoch, Germany) and the median growth-inhibition concentration (IC_{50}) was determined according to the formula (1), the results were shown as the median ±SD.

Cell death (%) = 100 – [(OD sample X 100)/OD control]

5.3. Determination of Apoptosis

The apoptosis induction potential was evaluated by the apoptosis detection kit (Biolegend, Germany) according to the manufacturer's guidelines. After 24 h lesinurad exposure, cells were trypsinized and washed with PBS (1X). Cells were resuspended in binding buffer (100 µL), annexin V and PI dyes were added to each sample and incubated at RT for 15 min. After Annexin V binding buffer (400 µL) was added, the fluorescence signal was measured in FITC and PE channels using ACEA flow cytometer (San Diego, CA, USA).

5.4. Determination of oxidative stress

5.4.1. *Reactive oxygen species (ROS) level*

The induction of ROS production was evaluated by comparing ROS levels in the exposed groups to the control ones. For that, a 2', 7'-dichlorofluorescein diacetate dye (H2DCF-DA) assay was applied and measured by flow cytometry. After drug treatment, cells were collected with trypsinization, washed with PBS (1X), 20 µM H2DCF-DA was added, and incubated at 37°C for 0.5 h. Then, cells were washed with

PBS (1X) and suspended in 1% of bovine serum albumin. The fluorescence signal was measured using ACEA flow cytometer (USA). The results were analyzed by NovoExpress Software (ACEA Biosciences, USA) and represented as mean ± SD fluorescence intensity.

5.4.2. Lipid peroxidation level

Lipid peroxidation was evaluated spectrophotometrically as previously stated by Buege and Aust (1978) based upon the formation of thiobarbituric acid-MDA adduct [34]. 1,1,3,3-tetraethoxypropane was used as the standard for the calculation of MDA levels in the cells. The protein level of each sample was measured with a BCA assay kit (Thermo Scientific Inc, USA). The MDA level of the cells was shown as µg MDA/mg protein in the samples.

5.4.3. Total antioxidant capacity (TAC) level

Antioxidant defense of the cells plays an important role in scavenging reactive oxygen species and other oxidative molecules. TAC level is a marker of antioxidant defense [35], for that, it was used in the study to evaluate the changes in the cellular antioxidant system. TAC level was determined with a commercial kit (Sigma, USA) following the manufacturer's rules. $1x10^4$ cells/well were seeded into a 96-well plate. After lesinurad treatment, the TAC level was determined using the upper phase (the cell culture medium) for the experiment. Trolox was used as a standard for the calculation of the TAC level of cells. ODs were read at 570 nm in a microwell plate reader (Epoch, Germany). The results were presented as nmol/ µL.

5.5. Determination of NF-κB protein level

The expression levels of NF-κB were examined with western blotting. The cellular proteins were extracted utilizing RIPA buffer (Santa Cruz Biotechnology, USA). Proteins were separated by sodium dodecyl sulfate-polyacrylamide gel electrophoresis (SDS-PAGE) and then, proteins were transferred to 0.22 µm nitrocellulose membrane (Biorad, USA) and the membranes were blocked with 5% non-fat dry milk. After blocking, membranes were incubated with primary antibody (ab16502, Abcam, UK, 1:1000 dilution) at +4 °C. After that, it was treated with HRP-conjugated secondary antibody (ab97051, Abcam, UK, 1:20.000 dilution). β-actin was utilized as a loading control (sc-47778, Santa Cruz Biotechnology, USA, 1:5000 dilution). The membranes were imaged with ECL substrate reagent (Thermo Scientific Inc., USA) in Fx-Vilber Lourmat (France). Results were calculated using Image J software and normalized to the control group.

5.6. Determination of Cytokine Levels

LEGENDplexTM Human Inflammation Panel (BioLegend, CA, USA) was utilized for the evaluation of TNF-α, IL-10, IL-6, and IL-2 secretion following the manufacturer's rules using FACS Calibur flow cytometer (BD Biosciences, CA, USA) in cell culture medium. The results were analyzed by LEGENDplex v8.0 software (BioLegend CA, USA). ConA, a plant lectin, has been demonstrated to induce cytokine release *in vivo* and *in vitro* [36, 37]. For that, ConA was employed as a positive control for the assay; Cells were treated with lesinurad at concentrations between 12.5 and 100 µM. Additionally, according to the results and to evaluate the ability of lesinurad to decrease the ConA-induced inflammation cells were pre-treated with ConA (25 µg/mL in PBS) for 12h, and then cells were exposed to lesinurad at 100 µM concentration.

5.7. Molecular Docking Studies

5.7.1. Ligand and protein preparation

Using the Maestro build panel and the LigPrep v2.5 module (Schrödinger LLC, New York, 2021-3), the chemical structures of lesinurad and reference ligands were built and prepared, respectively. The preparation step involved generating lower energy conformers at the OPLS4 force field of all compounds. Also, the ionized were generated states at target pH 7.0 ± 2.0 using the Epik 2.0. All other parameters were set to their default value [38].

The X-ray structure of TACE protein complexed with IK-682 (PDB code: 2FV5, resolution = 2.10 Å) and lectin concanavalin a (Con a) complexed with α-methyl-D-mannopyranoside (PDB code: 5CNA, resolution = 2.00 Å) was extracted from the Protein Data Bank (PDB). Then, all the obtained crystal structures were processed by the Protein Preparation Wizard tool projected in the Maestro program [39]. During the protein preparation step, the hydrogens were added to heavy atoms, the missing side chains were filled using Prime, the charges and bond orders were assigned, all water molecules were removed

beyond 3 Å from the hit group, and finally, the protein structures were minimized using the OPLS4 force field. This was followed by generating the receptor grid for docking using the receptor grid generation tool in Maestro.

5.7.2. XP Glide Docking

The extra precision flexible ligand docking mode was applied using the Glide tool of maestro Schrödinger 2021-3. The Van der Waals scaling factor and the partial charge cutoff for ligand atoms were selected to be 0.80 and 0.15, respectively [40]. The final scoring was carried out on energy minimized pose and was recorded as a Glide score, which indicates the binding affinity of the compound with the target protein. Higher scores indicate stronger binding. Moreover, the Glide scoring function score (Glide Gscores) and glide's empirical scoring function (glide emodel) values were examined that reflect the predicted binding free energy of the compound with the target protein and the predicted ligand-receptor interaction energy, respectively. The obtained pose that presented the least glide score (higher in negative value) was selected as the best pose and labelled for each ligand.

5.8. MM-GBSA:

The Molecular Mechanics-Generalized Born Surface Area (MM-GBSA) approach has recently garnered attention in drug discovery as a valuable tool for estimating the relative binding free energies of investigated hit structures [41, 42]. In this work, we report the assessment of molecular docking scores obtained for the lesinurad, ik-682, and α-methyl-D-mannopyranoside candidates, along with their corresponding MM-GBSA scoring values for two tested target proteins, Con a and TACE. The MM-GBSA scoring study was conducted using the Schrodinger suite of software (Maestro, version 2021-3) employing the OPLS4 force field. The binding free energy, ΔG_{bind}, was estimated as follows:

$\Delta G_{bind} = \Delta E_{MM} + \Delta G_{solv} + \Delta G_{SA}$

Where ΔE_{MM} represents the energy gap between the ligand-protein complex and the cumulative energy of the ligand and target protein in their uncomplexed state, ΔG_{solv} is the energy difference between the GBSA solvation energy of the complex and the comprehensive solvation energies of the unliganded protein target and the candidate ligand, and ΔG_{SA} refers to the surface area energy variance between the complex and the total surface area energies calculated for the uncomplexed protein and ligand.

Acknowledgments: The author(s) received no financial support for the research, authorship, and/or publication of this article.

Author contributions: Concept – T.B., M.A; Design – T.B., M.A.; Supervision – T.B., M.A.; Resources – T.B., M.A.; Materials – T.B., M.A., M.T.Q; Data Collection and/or Processing – T.B., M.A., M.T.Q; Analysis and/or Interpretation – T.B., M.A., M.T.Q; Literature Search – T.B., M.A., M.T.Q; Writing – T.B., M.A., M.T.Q; Critical Reviews – T.B., M.A., M.T.Q

Conflict of interest statement: The authors declared no conflict of interest.

REFERENCES

[1] Li X, Yan Z, Carlström M, Tian J, Zhang X, Zhang W, Wu S, Ye F. Mangiferin ameliorates hyperuricemic nephropathy which is associated with the downregulation of AQP2 and increased urinary uric acid excretion. Front Pharmacol. 2020; 11: 49. https://doi.org/10.3389/fphar.2020.00049

[2] Miner JN, Tan PK., Hyndman D, Liu S, Iverson C, Nanavati P, Hagerty DT, Manhard K, Shen Z, Girardet JL, Yeh L, Terkeltaub R, Quart B. Lesinurad, a novel, oral compound for gout, acts to decrease serum uric acid through inhibition of urate transporters in the kidney. Arthritis Res Ther. 2016; 18(1): 1-10. https://doi.org/10.1186/s13075-016-1107-x.

[3] FDA 2015, Highlights of prescribing information for Zurampic (Reference ID: 3864748). Revised in 12/2015. https://www.accessdata.fda.gov/drugsatfda_docs/label/2015/207988lbl.pdf.

[4] EMA 2016, EPAR summary for the public for Zurampic (EMEA/H/C/003932). updated in 02/2016. https://www.ema.europa.eu/en/documents/overview/zurampic-epar-summary-public_en.pdf. (accessed on 19 May 2022).

[5] Sam SE, Thomas TE, Abraham, E. A Review on gout. World J Pharm Res 2016; 5(6): 634-647.

[6] Robinson PC. Gout–An update of aetiology, genetics, co-morbidities and management. Maturitas. 2018; 118: 67-73. https://doi.org/10.1016/j.maturitas.2018.10.012

[7] Huneycutt E, Board C, Clements JN. Lesinurad, a selective URAT-1 inhibitor with a novel mechanism in combination with a xanthine oxidase inhibitor, for hyperuricemia associated with gout. J Pharm Pract. 2018;31(6):670-677. https://doi.org/10.1177/0897190017734427

[8] Abhishek A. New urate-lowing therapies. BMC Pharmacol Toxicol. 2018; 30(2): 177-182. https://doi.org/10.1097/bor.0000000000000476

[9] FDA Cross-Discipline Team Leader Review, 2014. https://www.accessdata.fda.gov/drugsatfda_docs/nda/2015/207988Orig1s000CrossR.pdf.

[10] Reddy ARN, Reddy YN, Krishna DR, Himabindu, V. Multi wall carbon nanotubes induce oxidative stress and cytotoxicity in human embryonic kidney (HEK-293) cells. Toxicology. 2010; 272(1-3): 11-16. https://doi.org/10.1016/j.tox.2010.03.017

[11] Reshma VG, Mohanan PV. Cellular interactions of zinc oxide nanoparticles with human embryonic kidney (HEK-293) cells. Colloids Surf B Biointerfaces. 2017; 157: 182-190. https://doi.org/10.1016/j.colsurfb.2017.05.069

[12] Ma Z, Cao X, Guo X, Wang M, Ren X, Dong R, Shao R, Zhu Y. Establishment and validation of an in vitro screening method for traditional chinese medicine-induced nephrotoxicity. Evid Based Complement Alternat Med. 2018; 5: 1-15. https://doi.org/10.1155/2018/2461915

[13] Goldfeld AE, Strominger JL, Doyle C. Human tumor necrosis factor alpha gene regulation in phorbol ester stimulated T and B cell lines. J Exp Med. 1991; 174(1): 73-81. https://doi.org/10.1084/jem.174.1.73

[14] Tracey KJ, Cerami DA. Tumor necrosis factor: A pleiotropic cytokine and therapuetic target. Annu Rev Med. 1994; 45(1): 491-503. https://doi.org/10.1146/annurev.med.45.1.491

[15] Zhang C, Lovering F, Behnke M, Zask A, Sandanayaka V, Sun L, Zhu Y, Xu W, Zhang Y, Levin J. Synthesis and activity of quinolinylmethyl P1′ α-sulfone piperidine hydroxamate inhibitors of TACE. Bioorg Med Chem Lett. 2009; 19(13): 3445-3448. https://doi.org/10.1016/j.bmcl.2009.05.020

[16] Kakizoe T, Komatsu H, Niijima T, Kawachi T, Sugimura T. Increased agglutinability of bladder cells by concanavalin A after administration of carcinogens. Cancer Res. 1980; 40(6): 2006-2009.

[17] Kanellopoulos JM, De Petris S, Leca G, Crumpton MJ. The mitogenic lectin from *Phaseolus vulgaris* does not recognize the T3 antigen of human T lymphocytes. Eur J Immunol. 1985; 15(5): 479-486. https://doi.org/10.1002/eji.1830150512

[18] Yu M, Sato H, Seiki M, Thompson EW. Complex regulation of membrane-type matrix metalloproteinase expression and matrix metalloproteinase-2 activation by concanavalin A in MDA-MB-231 human breast cancer cells. Cancer Res. 1995; 55(15): 3272-3277.

[19] Lei HY, Chang CP. Lectin of Concanavalin A as an anti-hepatoma therapeutic agent. J Biomed Sci. 2009; 16(1): 1-12. http://dx.doi.org/10.1186/1423-0127-16-10

[20] Murumkar PR, Sharma MK, Giridhar R, Yadav MR. Virtual screening-based identification of lead molecules as selective TACE inhibitors. Med Chem Res. 2015; 24: 226-244. https://doi.org/10.1007/s00044-014-1097-7

[21] Wu Z, Thiriot DS, Ruoho AE. Tyr199 in transmembrane domain 5 of the β2-adrenergic receptor interacts directly with the pharmacophore of a unique fluorenone-based antagonist. Biochem J. 2001; 354(3): 485-491. https://doi.org/10.1042/bj3540485

[22] Klein RW, Kabadi S, Cinfio FN, Bly CA, Taylor DC, Szymanski KA. Budget impact of adding lesinurad for second-line treatment of gout: A US health plan perspective. J Comp Eff Res. 2018; 7(8): 807-816. https://doi.org/10.2217/cer-2017-0103

[23] Ben Salem C, Slim R, Fathallah N, Hmouda H. Drug-induced hyperuricaemia and gout. Rheumatology. 2017; 56(5): 679-688. https://doi.org/10.1093/rheumatology/kew293

[24] Verzola D, Ratto E, Villaggio B, Parodi EL, Pontremoli R, Garibotto G, Viazzi F, Franco M. Uric acid promotes apoptosis in human proximal tubule cells by oxidative stress and the activation of NADPH oxidase NOX 4. PloS one. 2014; 9(12): e115210. https://doi.org/10.1371/journal.pone.0115210

[25] Heitel P, Gellrich L, Heering J, Goebel T, Kahnt A, Proschak E, Schubert-Zsilavecz M, Merk D. Urate transporter inhibitor lesinurad is a selective peroxisome proliferator-activated receptor gamma modulator (sPPARγM) in vitro. Sci Rep. 2018; 8(1): 1-11. https://doi.org/10.1038/s41598-018-31833-4.
[26] Sánchez-Lozada LG, Soto V, Tapia E, Avila-Casado C, Sautin YY, Nakagawa T, Rodríguez-Iturbe B, Johnson RJ. Role of oxidative stress in the renal abnormalities induced by experimental hyperuricemia. Am J Physiol Renal Physiol. 2008; 295(4): F1134-F1141. https://doi.org/10.1152/ajprenal.00104.2008
[27] Alghamdi YS, Soliman MM, Nassan MA. Impact of Lesinurad and allopurinol on experimental hyperuricemia in mice: biochemical, molecular and immunohistochemical study. BMC Pharmacol Toxicol. 2020; 21(1): 10. https://doi.org/10.1186/s40360-020-0386-7
[28] Lee YS, Sung YY, Yuk HJ, Son E, Lee S, Kim JS, Kim DS. Anti-hyperuricemic effect of *Alpinia oxyphylla* seed extract by enhancing uric acid excretion in the kidney. Phytomedicine. 2019; 62: 152975. https://doi.org/10.1016/j.phymed.2019.152975
[29] Navarro-González JF, Mora-Fernández C. The role of inflammatory cytokines in diabetic nephropathy. J Am Soc Nephrol. 2008; 19: 433-442. https://doi.org/10.1681/ASN.2007091048.
[30] Zhang H, Sun SC. NF-KB in inflammation and renal diseases. Cell Biosci. 2015; 5:63. https://doi.org/10.1186/s13578-015-0056-4
[31] Liu T, Zhang L, Joo D, Sun SC. NF-κB signaling in inflammation. Signal Transduc Target Ther. 2017; 2: 17023. https://doi.org/10.1038/sigtrans.2017.23
[32] Gillen M, Yang C, Wilson D, Valdez S, Lee C, Kerr B, Shen Z. Evaluation of pharmacokinetic interactions between lesinurad, a new selective urate reabsorption inhibitor, and CYP enzyme substrates sildenafil, amlodipine, tolbutamide, and repaglinide. Clin Pharmacol Drug Dev. 2017; 6(4): 363-376. https://doi.org/10.1002/cpdd.324.
[33] Fotakis G, Timbrell JA. In vitro cytotoxicity assays: comparison of LDH, neutral red, MTT and protein assay in hepatoma cell lines following exposure to cadmium chloride. Toxicol Lett. 2006; 160(2): 171-177. https://doi.org/10.1016/j.toxlet.2005.07.001
[34] Buege JA, Aust SD. Microsomal lipid peroxidation. Methods Enzimol. 1978; 52: 302-310. https://doi.org/10.1016/S0076-6879(78)52032-6
[35] Bucalen CF. Effects of xenobiotics on total antioxidant capacity. Interdiscip Toxicol. 2012; 5(3): 117-122. https://doi.org/10.2478/v10102-012-0019-0
[36] Sharma R, Tiku AB. Emodin inhibits splenocyte proliferation and inflammation by modulating cytokine responses in a mouse model system. J Immunotoxicol. 2016; 13(1): 20-26. https://doi.org/10.3109/1547691x.2014.995243.
[37] Chae BS. Pretreatment of low-dose and super-low-dose LPS on the production of in vitro LPS-induced inflammatory mediators. Toxicol Res. 2018; 34(1): 65-73. https://doi.org/10.5487/tr.2018.34.1.065.
[38] Shelley JC, Cholleti A, Frye LL, Greenwood JR, Timlin MR, Uchimaya M. Epik: a software program for pK a prediction and protonation state generation for drug-like molecules. J Comput Aided Mol Des.2007; 21(12): 681-691. https://doi.org/10.1007/s10822-007-9133-z.
[39] Protein Preparation Wizard; Epik, Schrödinger, LLC, New York, NY, 2021.
[40] Friesner RA, Murphy RB, Repasky MP, Frye LL, Greenwood JR, Halgren TA, Sanschhagrin PC, Mainz DT. Extra precision glide: Docking and scoring incorporating a model of hydrophobic enclosure for protein− ligand complexes. J Med Chem. 2006; 49(21): 6177-6196. https://doi.org/10.1021/jm051256o.
[41] Li J, Abel R, Zhu K, Cao Y, Zhao S, Friesner RA. The VSGB 2.0 model: a next generation energy model for high resolution protein structure modeling. Proteins. 2011; 79(10): 2794-2812. https://doi.org/10.1002/prot.23106.
[42] Zamzami MA. Molecular docking, molecular dynamics simulation and MM-GBSA studies of the activity of glycyrrhizin relevant substructures on SARS-CoV-2 RNA-dependent-RNA polymerase. J Biomol Struct Dyn. 2023; 41(5): 1846-1858. https://doi.org/10.1080/07391102.2021.2025147.